


ORIGINAL ARTICLE

A novel mutation in *PLS3* causes extremely rare X-linked osteogenesis imperfecta

Jing Hu¹ | Lu-jiao Li^{1,2} | Wen-bin Zheng¹ | Di-chen Zhao¹ | Ou Wang¹ | Yan Jiang¹ | Xiao-ping Xing¹ | Mei Li¹  | Weibo Xia¹

¹Department of Endocrinology, National Health Commission Key Laboratory of Endocrinology, Peking Union Medical College Hospital, Chinese Academy of Medical Sciences and Peking Union Medical College, Beijing, China

²Department of Endocrinology, Beijing Friendship Hospital, Capital Medical University, Beijing, China

Correspondence

Mei Li and Weibo Xia, Department of Endocrinology, Key Laboratory of Endocrinology, National Health and Family Planning Commission, Peking Union Medical College Hospital, Chinese Academy of Medical Sciences and Peking Union Medical College, Shuaifuyuan No. 1, Dongcheng District, Beijing 100730, China.

Email address: limeilzh@sina.com (M. L.) and xiaweibo8301@163.com (W. X.)

Funding information

Chinese Academy of Medical Sciences Innovative Fund for Medical Sciences (CIFMS), Grant/Award Number: 2016-I2M-3-003; Beijing Natural Science Foundation, Grant/Award Number: 7202153; National Natural Science Foundation of China, Grant/Award Number: 81873668; National Key Research and Development Program of China, Grant/Award Number: 2018YFA0800801

Abstract

Background: Osteogenesis imperfecta (OI) is a phenotypically and genetically heterogeneous bone disease characterized by bone fragility and recurrent fractures. X-linked inherited OI with mutation in *PLS3* is so rare that its genotype–phenotype characteristics are not available.

Methods: We designed a novel targeted next-generation sequencing (NGS) panel with the candidate genes of OI to detect pathogenic mutations and confirmed them by Sanger sequencing. The phenotypes of the patients were also investigated.

Results: The proband, a 12-year-old boy from a nonconsanguineous family, experienced multiple fractures of long bones and vertebrae and had low bone mineral density (BMD Z-score of -3.2 to -2.0). His younger brother also had extremity fractures. A novel frameshift mutation (c.1106_1107insGAAA; p.Phe369Leufs*5) in exon 10 of *PLS3* was identified in the two patients, which was inherited from their mother who had normal BMD. Blue sclerae were the only extraskeletal symptom in all affected individuals. Zoledronic acid was beneficial for increasing BMD and reshaping the compressed vertebral bodies of the proband.

Conclusion: We first identify a novel mutation in *PLS3* that led to rare X-linked OI and provide practical information for the diagnosis and treatment of this disease.

KEYWORDS

novel mutation, *PLS3*, treatment, X-linked osteogenesis imperfecta

Jing Hu and Lu-jiao Li contribute equally to this work and list as the co-first-author.

This is an open access article under the terms of the Creative Commons Attribution-NonCommercial-NoDerivs License, which permits use and distribution in any medium, provided the original work is properly cited, the use is non-commercial and no modifications or adaptations are made.

© 2020 The Authors. *Molecular Genetics & Genomic Medicine* published by Wiley Periodicals LLC.

1 | INTRODUCTION

Osteogenesis imperfecta (OI), a heritable bone disorder with an incidence of 1:15,000 to 1:20,000 live births, is mainly caused by mutations in genes involved in type I collagen synthesis, processing, secretion, and posttranslational modification and in the regulation of osteoblast function (Folkestad et al., 2016; Tauer et al., 2019). Frequent bone fractures and skeletal deformity are the hallmarks of OI, while some patients also have extraskeletal manifestations, such as blue sclerae, dentinogenesis imperfecta, hearing impairment, or joint laxity (Bardai et al., 2017; Marini et al., 2017). Mutations in the *COL1A1* and *COL1A2* genes, which encode the $\alpha 1$ and $\alpha 2$ chains of type I collagen, respectively, are found in 85%–90% patients with OI, which is consistent with autosomal dominant inheritance (Besio et al., 2019; Marini et al., 2017). However, mutations in other causative genes of OI can cause collagen defects through distinct mechanisms (Besio et al., 2019; Tauer et al., 2019; Webb et al., 2017).

In 2013, mutations in *PLS3* were identified in five families with X-linked osteoporosis (van Dijk et al., 2013). *PLS3* (OMIM 300131), which is located on chromosome Xq23 and has 16 exons, is ubiquitously expressed in solid tissues and involved in the dynamic assembly and disassembly of actin bundles in the cytoskeleton (Delanote et al., 2005). The underlying molecular mechanism for its roles in the regulation of skeletal development remains unknown (Kamioka et al., 2004; Tanaka-Kamioka et al., 1998). More recently, *PLS3* has been suggested to have a role in the mineralization process. Patients with *PLS3* mutation present with recurrent fractures and rarely have extraskeletal manifestations of OI (Balasubramanian et al., 2018; Collet et al., 2018; Costantini, et al., 2018; Costantini, et al., 2018; van Dijk et al., 2013; Fahiminiya et al., 2014; Kampe et al., 2017; Kampe et al., 2017; Kannu et al., 2017; Laine et al., 2015; Lv et al., 2017; Nishi et al., 2016; Wang et al., 2020). Because of its X-linked inheritance, *PLS3*-induced OI is more severe in men than in women (Cao et al., 2019; Chen et al., 2018; van Dijk et al., 2013; Fahiminiya et al., 2014; Kampe et al., 2017; Kannu et al., 2017; Laine et al., 2015; Lv et al., 2017; Wang et al., 2020). However, a full understanding of the skeletal disease associated with the *PLS3* mutation was hampered by its extremely low incidence, genotypic heterogeneity, and phenotypic diversity.

In the present study, we detected a pathogenic mutation in a nonconsanguineous family with X-linked OI and summarized previous literature on the clinical characteristics of patients with *PLS3* mutation to explore the genotype–phenotype correlation of this rare disorder.

2 | MATERIALS AND METHODS

2.1 | Ethical compliance

The study was approved by the Scientific Ethnic Committee of Peking Union Medical College Hospital (PUMCH). The procedures used in this study adhere to the tenets of the Declaration of Helsinki. Informed consent was provided by the parents before participation in the study.

2.2 | Subjects

The proband of Han nationality, who complained of back pain for 4 months, was recruited by the Endocrinology Department, Peking Union Medical College Hospital (PUMCH), in 2018. His younger brother visited the clinic due to recurrent fractures. These two patients were suspected of having OI. Both brothers and their parents were included in the study.

2.3 | Clinical evaluation

Clinical data were thoroughly collected, including fracture history, growth and development speed, and family history. The participants also underwent a detailed physical examination, including the sclerae, teeth, and muscular and skeletal systems. The heights and weights of the patients were measured by a Harpenden stadiometer (Seritex Inc., East Rutherford, NJ), and age- and sex-specific Z-scores of height and weight were calculated on the basis of Chinese national growth standards (Li et al., 2009; Song et al., 2016).

Serum levels of calcium (Ca), phosphorus (P), 25-hydroxyvitamin D (25OHD), alkaline phosphatase (ALP, a bone formation marker), alanine aminotransferase (ALT), and creatinine (Cr) were measured by a fully automated chemical analyzer (ADVIA[®] 1800, Siemens Inc., Germany). Serum levels of cross-linked C-telopeptide of type I collagen (β -CTX, a bone resorption marker) and intact parathyroid hormone (PTH) were quantified using an automated Roche electrochemiluminescence system (Roche Diagnostics, Switzerland). All biochemical indices were measured in the central laboratory of PUMCH.

Dual-energy X-ray absorptiometry (DXA, GE-Lunar Prodigy Advance) was utilized to measure the bone mineral densities (BMDs) of the lumbar spine (L1–L4) and proximal hip of the patients. The results were then transformed to age- and sex-matched Z-scores according to the BMD data in normal Chinese and Asian children (Khadilkar et al., 2011). Radiographs of the skull, extremities, and thoracolumbar spine

were examined. The Genant semiquantitative method was used for the radiographic diagnosis of vertebral compression fractures (VCFs), where a VCF was defined as more than a 20% reduction in any vertebral height (Genant et al., 1993).

2.4 | Identification and confirmation of the pathogenic mutation

Genomic DNA of the participants was extracted from peripheral leukocytes by a standard procedure using a QIAamp DNA Mini Kit (Qiagen, Germany). To identify the likely deleterious mutation, gDNA of the proband and his brother was sequenced using a targeted next-generation sequencing (NGS) panel (Illumina HiSeq2000 platform, Illumina, Inc., San Diego, CA, USA), which covered 822 genes implicated in hereditary bone diseases, including the pathogenic genes of OI (*COL1A1*, *COL1A2*, *IFITM5*, *PPIB*, *PLS3*, *SERPINF1*, *SERPINH1*, *PLOD2*, *CRTAP*, *LEPRE1*, *FKBP10*, *SP7*, *BMP1*, *TMEM38B*, *WNT1*, *LRP5*, *CREB3L1*, *P4HB*, *SEC24D*, *SPARC*, *TMEM38B*, and *MBTPS2*). The overall sequencing coverage of the target regions was >95% at a minimum of 20× sequencing depth.

Burrows-Wheeler Aligner software was used to align the sequence to the human genome (NCBI37/hg19), and SOAP SNP software was used to identify the single nucleotide variants (SNVs) (Richards et al., 2008). We filtered out mutations with an allele frequency $\geq 1\%$ in dbSNP, HapMap, 1000G ASN AF, ESP6500 AF, ExAC, and 1000 Genomes, and the pathogenicity of the mutation was further evaluated using Mutation Taster (<http://www.mutationtaster.org>).

Mutation in *PLS3* was confirmed in the brothers and their mother by Sanger sequencing. Exon 10 of *PLS3* was amplified by polymerase chain reaction (PCR) under the following conditions: initial denaturation at 95°C for 3 min, followed by 35 cycles at 95°C for 30 s, 58.5–61.5°C for 30 s, and 72°C for 40–100 s. The specific primers from the genomic sequence (NG_012518.2) were designed using web-based Primer 3 (<http://bioinfo.ut.ee/primer3-0.4.0/>), and their sequences were as follows: 5'-GACTATGACAGTGGGAAATTTCTA-3' for the forward primer and 5'-CCACACATTCGAAATTGAGGTT-3' for the reverse primer. PCR products were purified and then sequenced by an ABI 377 DNA-automated sequencer with dye terminator cycle sequencing kits (Applied Biosystems). Sequencing traces were aligned with NCBI reference sequence of *PLS3* (NM_001136025.5).

2.5 | Treatment and follow-up

The two patients received once-yearly intravenous infusion of zoledronic acid 5 mg (Aclasta[®], Novartis Pharma

Schweiz AG, Switzerland). Calcium at 600 mg plus 125 IU vitamin D3 (Caltrate D Wyeth Pharmaceuticals, USA) and calcitriol 0.25 µg (Rocaltrol, R.P. Scherer GmbH & Co. KG, Germany) were prescribed daily for the proband, whereas his brother was supplemented with a half dose of calcium plus vitamin D3 and calcitriol. The treatment duration was 2 years. To evaluate the therapeutic effects, changes in bone turnover biomarkers and BMD were measured.

2.6 | Analysis of the clinical characteristics of previously reported patients with *PLS3* mutations

An electronic literature search was further conducted in Medline via the PubMed, Embase, and Web of Science databases to summarize the clinical characteristics of patients with *PLS3* mutation, and the keywords for searching included 'plastin 3' and 'PLS3' in combination with 'osteogenesis imperfecta' and 'osteoporosis'. No limits were placed on publication year or language. A total of 24 families from 15 studies were collected for analysis. Available data on clinical evaluations, genetic findings, and therapeutic features were extracted and summarized.

3 | RESULTS

3.1 | Phenotypes of the patients

The proband, a 12-year-old boy, was the first child of a non-consanguineous family. He was delivered vaginally at term with a birth weight of 3550 g. His cognitive and motor development were normal. He experienced a low-trauma fracture of the right forearm at 4 years old. Notably, he suffered from back pain due to falling from a standing height 4 months before he visited PUMCH. Physical examination indicated blue sclerae and kyphosis, with normal joint laxity, dentition, and hearing. He had a normal height of 153 cm (Z-score 0.15) but was overweight with a body mass index of 27.3 kg/m² (higher than the 97th percentile) (Song et al., 2016). Serum concentrations of calcium, phosphate, ALP, and PTH were within normal age-specific ranges. The proband had vitamin D deficiency and an elevated level of serum ALT. Since the normal range of β -CTX was unavailable in Chinese children, we could not evaluate whether his β -CTX level was normal. He had low BMDs at the lumbar spine of 0.480 g/cm² (L1-L4 Z-score -2.0) and femoral neck of 0.588 g/cm² (Z-score -3.2). X-ray films revealed severe compression fractures in the thoracic and lumbar vertebrae. Slender long bones with thin cortices and Wormian bones were also observed (Figures 1 and 2).

The 6-year-old brother of the proband visited our clinic at the same time. He was born full-term via spontaneous

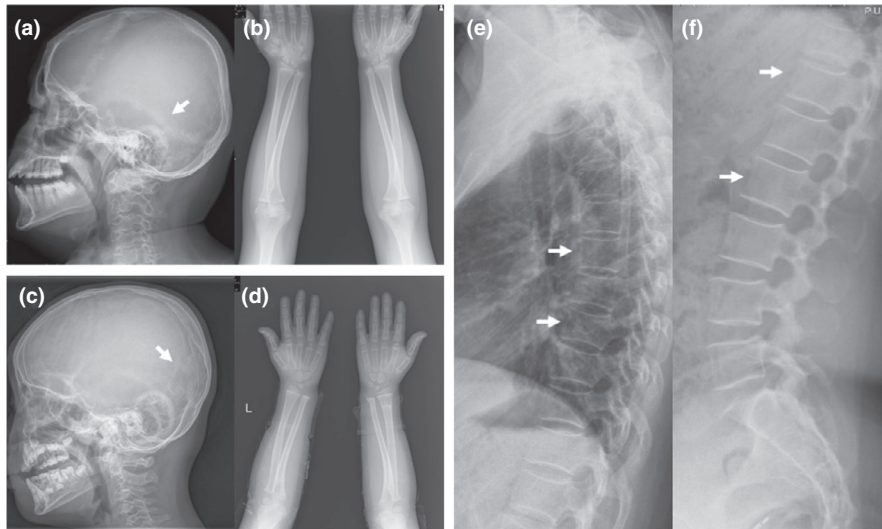


FIGURE 1 Skeletal radiographs of the two boys and their mother at the first evaluation. (a) Lateral cephalogram of the proband; (b) Wormian bone in the skull pointed out by an arrow; Anteroposterior radiograph of the forearm of the proband slender long bone with thin cortices; (c) Lateral cephalogram of the younger brother Wormian bone in the skull marked with an arrow; (d) Anteroposterior radiograph of the forearm of the younger brother slender long bone with thin cortices; (e) Lateral thoracic X-ray of the mother reduced bone mineral density and thin cortices without VCFs; (f) Lateral lumbar X-ray of the mother reduced bone mineral density and thin cortices without VCFs

vaginal delivery with a high birth weight (4500 g), and his development was unremarkable. Fragility fractures of his right forearm and right radius occurred at 5 years old. He had blue sclerae but normal teeth, gait pattern, and joint mobility. He had a normal height of 120 cm (Z-score 0.49) and a normal weight of 27 kg (Z-score 1.88) for his age. Serum levels of calcium, phosphate, PTH, and ALT were normal, whereas vitamin D deficiency and an elevated level of ALP were found. The serum β -CTX level was 1.500 ng/ml. Although the BMDs of the lumbar spine (L1-L4: 0.529 g/cm², Z-score -0.2) and femoral neck (0.674 g/cm², Z-score 0.5) were normal, X-ray films demonstrated slender long bones with thin cortices, Wormian bones, and osteoporosis in the spine (Figures 1 and 2).

The mother of the patients had blue sclerae in the absence of other clinical manifestations. Furthermore, she had vitamin D insufficiency with normal bone turnover biomarkers. She had normal BMD, while X-ray revealed that she had osteoporosis (Figure 1). She and her siblings had not yet experienced bone fractures. The maternal grandfather of the proband had suffered from several fractures under minor force. More clinical features of the maternal family members were unavailable. The clinical manifestations of the brothers and the mother are shown in Table 1.

3.2 | Genetic findings

Sequence analysis revealed a novel frameshift mutation (c.1106_1107insGAAA) in exon 10 of *PLS3* in the proband, his brother, and mother. The mutation resulted

in a frameshift and early termination of mRNA translation (p.Phe369Leufs*5). Sanger sequencing confirmed that the proband and his brother were hemizygous, while his mother was heterozygous for the mutant *PLS3* (Figure 3). This variant in *PLS3* was not reported in the ExAC, 1000 Genomes, and PubMed databases, and was absent in our in-house exome database. The mutation was predicted to be deleterious with MutationTaster software. Moreover, the mutation would lead to nonsense-mediated mRNA decay (NMD). No mutations were found in other OI-related genes.

3.3 | Effects of BPs

After 24 months of bisphosphonate (BP) treatment, the serum β -CTX levels of the proband and his brother decreased by 8.3% and 17.3%, respectively. The BMD values of the proband were markedly increased by 96.9% (Z-score from -2.0 to 1.0) at the lumbar spine and 62.8% (Z-score from -3.2 to 1.0) at the femoral neck. The BMD values of his brother were increased by 74.3% (Z-score from -0.2 to 4.2) at the lumbar spine and 30.4% (Z-score from 0.5 to 1.8) at the femoral neck (Figure 4). No new fractures occurred in the proband or his brother during the 24-month intervention. Vertebral body height, also called reshaping of the vertebra, was significantly improved after the treatment (Figure 2).

The two patients had a mild fever within 2 or 3 days after initiation of zoledronic acid treatment. No other side effects were observed.

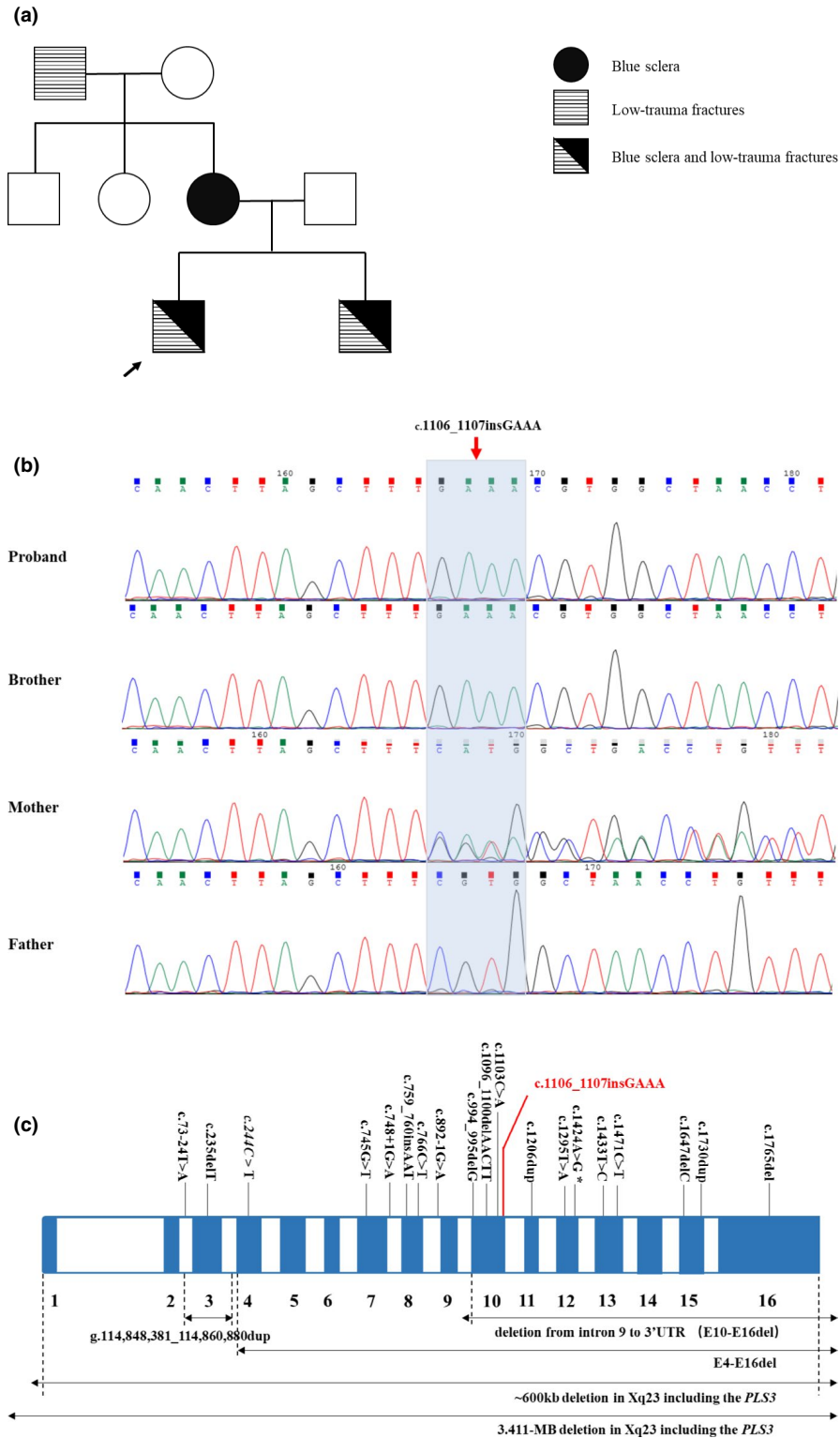


FIGURE 2 Lateral spinal X-ray at baseline, 6-, 12- and 24-month follow-up after zoledronate treatment. (a) Lateral spinal X-ray of the proband at baseline severe spinal osteoporosis with multiple vertebral fractures and kyphosis marked with arrows; (b) Lateral spinal X-ray of the proband at 6-month follow-up; (c) Lateral spinal X-ray of the proband at 12-month follow-up; (d) Lateral spinal X-ray of the proband at 24-month follow-up reshaping of the compressed vertebral body pointed out by arrows after the treatment; (e) Lateral spinal X-ray of the younger brother at baseline decreased bone density without VCFs; (f) Lateral spinal X-ray of the younger brother at 6-month follow-up; (g) Lateral spinal X-ray of the younger brother at 12-month follow-up; (h) Lateral spinal X-ray of the younger brother at 24-month follow-up increase in bone density and thicker cortices after the treatment

	Proband	Brother	Mother	Reference range
Age at the first visit (year)	12.6	6.0	36	/
Long-bone fracture	1	2	0	/
Vertebral compression fractures	Yes	No	0	/
Sclerae	Blue	Blue	Blue	/
Joint Hyperlaxity	No	No	No	/
Dentinogenesis Imperfecta	No	No	No	/
Hearing Loss	No	No	No	/
Height (cm)	153	120	160	/
Weight (kg)	64	27	63	/
LS BMD (g/cm ²)	0.480	0.529	1.129	/
LS BMD Z-score	-2.0	-0.2	-0.5	/
FN BMD (g/cm ²)	0.588	0.674	0.959	/
FN BMD Z-score	-3.2	0.5	0.2	/
TH BMD (g/cm ²)	0.534	0.644	0.917	/
TH BMD Z-score	-	-	-0.6	/
Ca (mmol/L)	2.45	2.49	2.30	2.13-2.70
P (mmol/L)	1.62	1.74	1.41	1.29-1.94; 0.81-1.45
β-CTX (ng/ml)	1.200	1.500	0.351	0.26-0.512
25OHD (ng/ml)	15.6	18.4	20.1	30-50
ALP (U/L)	384	416	NA	42-390; 50-135
PTH (pg/ml)	15.8	19.6	30.4	12.0-68.0
ALT (U/L)	78	11	10	9-50
Cr (μmol/L)	38	34	54	18-88

Abbreviations: 25OHD, 25-hydroxyvitamin D; ALP, alkaline phosphatase; ALT alanine aminotransferase; BMD, bone mineral density; Ca, calcium; Cr, creatinine; FN, femoral neck; LS, lumbar spine; P, phosphorus; PTH, parathyroid hormone; TH, total hip; β-CTX, cross-linked C-telopeptide of type I collagen.

3.4 | Phenotypes and genotypes of previously reported patients with *PLS3* mutation

The *PLS3* mutation was identified in at least 44 male patients from 25 families, including our patients (Table 2). These individuals all had reduced BMD and shared similar skeletal phenotypes; 40 of 43 patients had a history of low-impact peripheral fractures, and 33 of 42 patients suffered from VCFs. The age of patients at the first clinical fracture ranged from 2 to 33 years. Apart from vertebral abnormalities, leg length discrepancy was described in one patient, and dysmorphic facial features were reported in five patients (Costantini, et al., 2018; Kampe et al., 2017; Nishi et al., 2016). Most patients had normal heights. Typical extraskeletal symptoms were less common, including blue sclerae (seven patients) (Chen et al., 2018; Costantini, et al., 2018; Kampe et al., 2017; Nishi et al., 2016), ligamentous laxity (seven patients) (Cao et al., 2019; Costantini, et al., 2018; van Dijk et al., 2013; Kampe et al.,

TABLE 1 Clinical characteristics of patients at the first visit

2017; Kampe et al., 2017; Nishi et al., 2016), dentinogenesis imperfecta (one patient) (Kampe et al., 2017), and hearing loss (three patients) (Costantini, et al., 2018; Nishi et al., 2016). Two patients had a myopathic gait or waddling gait (van Dijk et al., 2013; Kampe et al., 2017). One patient with epilepsy and one patient with autism spectrum disorder (ASD) were reported. The clinical phenotypes of heterozygous female carriers were highly variable from normal BMD to severe osteoporosis with multiple fractures. Interestingly, a 10-year-old girl heterozygous for a de novo detrimental variant (c.1424A>G in exon 12) exhibited severe symptoms of recurrent fractures, VCFs, and extremely low BMD (Kampe et al., 2017).

In the studies linking *PLS3* to skeletal fragility, eight frameshift mutations (Families 1, 5, 9, 10, 13, 17, 20, and 25), five nonsense mutations (Families 2, 14, 15, 22, and 23), three splice-site variants (Families 3, 12, and 24), three missense mutations (Families 11, 18, and 21), and one insertion mutation (Family 4) were identified (Table 2 and Figure 2).

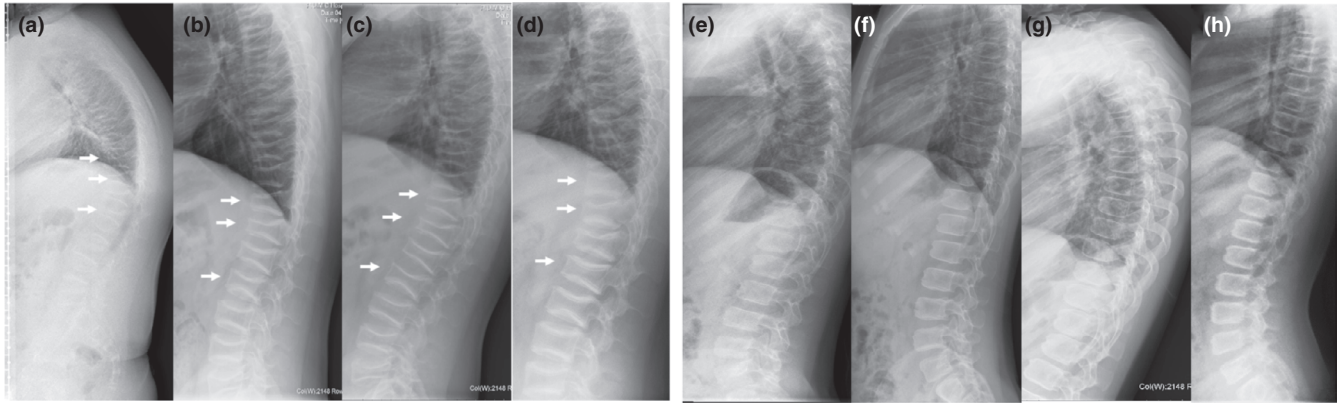


FIGURE 3 Pedigree of the family with X-linked osteogenesis imperfecta (OI) and genetic analysis of *PLS3*. (a) Pedigree of the affected family. The proband was indicated by an arrow. The mother of the proband and her siblings had no history of fractures. The maternal grandfather had a history of recurrent low-trauma fractures. The colors of sclerae were unknown in the maternal grandfather and the siblings of the mother since they were unavailable. (b) Sanger sequencing of four individuals in this family. The affected gene site was marked with shadow. (c) Distribution of pathogenic mutations associated with X-linked OI in *PLS3*. A mutation in *PLS3* found in a 10-year-old female was marked with an asterisks (*). The mutation (NCBI reference sequencing: NM_001136025.5) in the present study was highlighted in red with bold font

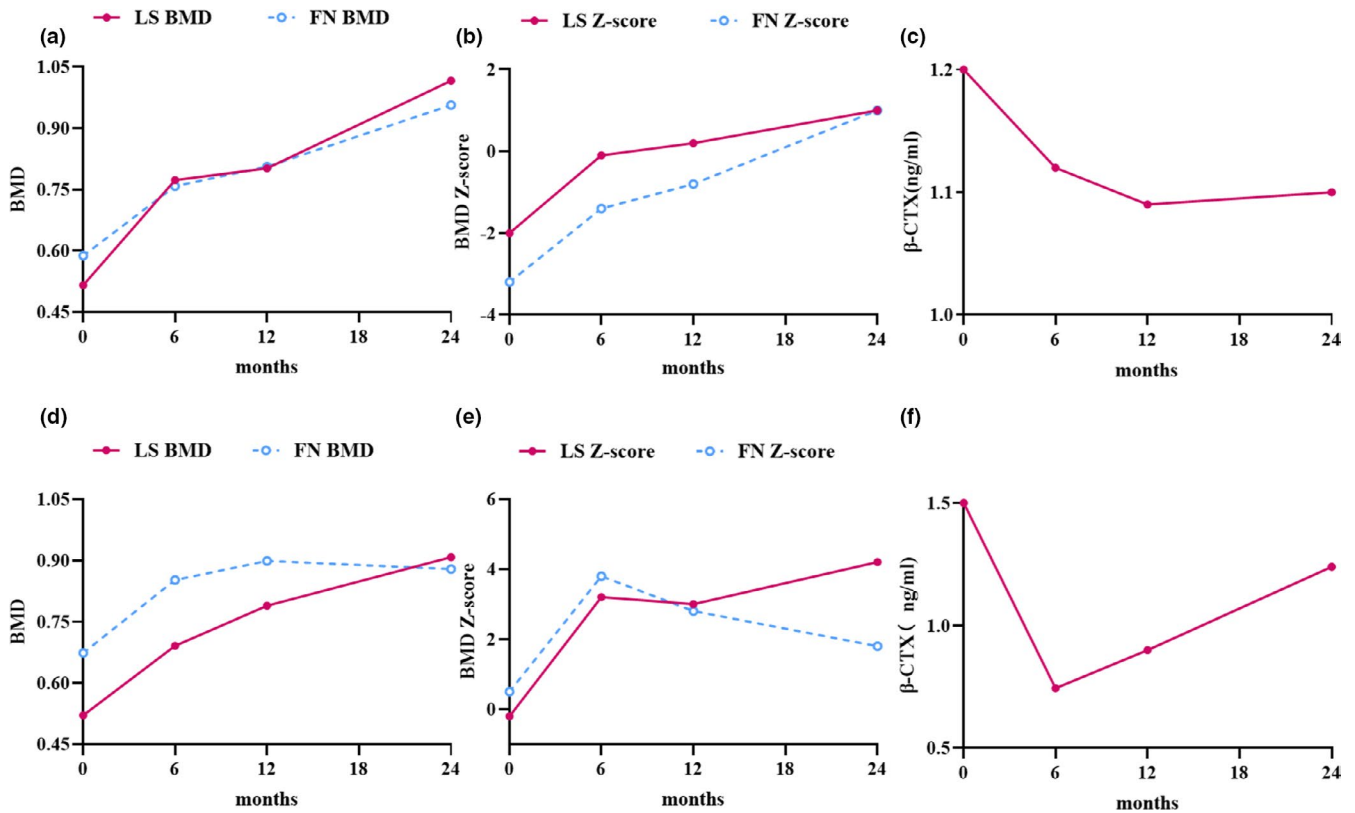


FIGURE 4 Changes in BMD, BMD Z-score and serum β -CTX level 0, 6 12 and 24 months after initiation of zoledronate treatment. (a) Changes in BMD at lumbar spine (LS) and femoral neck (FN) of the proband; (b) Changes in BMD Z-score at LS and FN of the proband; (c) Changes in serum β -CTX level of the proband over time; (d) Changes in BMD at LS and FN of the younger brother; (e) Changes in BMD Z-score at LS and FN of the younger brother; (f) Changes in serum β -CTX level of the younger brother over time

Variants were randomly distributed over 10 exons (exons 3, 4, 7, 8, 10, 11, 12, 13, 15, and 16) and three introns (introns 2, 7, and 8), without any obvious hotspot mutations (Figure 3).

Deletion or duplication of a large fragment was also found. However, phenotype–genotype correlations could not be well established in these patients.

TABLE 2 Clinical and molecular characteristics of previously reported male patients with *PLS3* mutation

Family no.	Number of male patients	Age at first fracture (years)	peripheral fracture(s)	VCFs/ number of patients	LS BMD Z-score (L1 to L4)	Extraskelletal manifestations/ number of patients ^a	Mutation type	Base change	Amino acid change	Treatment of BPs	Reference
1	6	2-8	Yes	Variable/2	-5.5 to -1.1	Variable/2	Frameshift	c.235delT in exon 3	P.Tyr79Ilefs*6	Yes	van Dijk et al. (2013)
2	2	7-10	Yes	Variable/1	-3.4 to -2.8	No	Nonsense	c.1471C>T in exon 13	p.Gln491*	Yes	van Dijk et al. (2013)
3	1	NA	NA	Yes	NA	No	Splice-site	c.748+1G>A in exon 7	p.Glu249_Ala250ins12	Yes	van Dijk et al. (2013)
4	1	NA	Yes	Yes	-2.5	No	Insertion	c.759_760insAAT in exon 8	p.Ala253_Leu254insAsn	Yes	van Dijk et al. (2013)
5	1	NA	Yes	Yes	-2.8	No	Frameshift	c.1647delC in exon 15	p.Ser550Alafs*9	Yes	van Dijk et al. (2013)
6	2	NA	No	Yes	-3.4	Variable/1	Deletion	E4-E16 del	NA	NA	Kampe et al. (2017)
7	1	4	Yes	Yes	-3.6	No	Deletion	E1-E16 del	NA	NA	Kampe et al. (2017)
8	1	4	Yes	Yes	-2.1	No	Deletion	g.112,419,139-115,830,286del	NA	Yes	Kannu et al. (2017)
9	1	2	Yes	Yes	-4.0	No	Frameshift	c.1730dup in exon 15	NA	Yes	Kannu et al. (2017)
10	2	2.2-2.5	Yes	Yes	-3.5 to -1.7	No	Frameshift	c.994_995delG in exon 10	p.Asp332*	Yes	Fahiminiya et al. (2014)
11	2	4.8-5	Yes	Yes	-3.3 to -3.4	No	Missense	c.1433T>C in exon 13	p.Leu478Pro	No	Fahiminiya et al. (2014)
12	6	7-33	Yes	Yes	-5.0 to -1.9	No	Splice-site	c.73-24T>A in intron 2	p.Asp25Alafs*17	Variable	Laine et al. (2015)
13	1	12	Yes	Yes	-4.8	No	Frameshift	c.1765del in exon 16	p.Ala589fs	Yes	Balasubramanian et al. (2018)
14	1	2	Yes	Yes	-2.7	NA	Nonsense	c.1295T>A in exon 12	p.Leu432*	Yes	Balasubramanian et al. (2018)
15	3	7 ^b	Yes	Variable/1	-4.8 to -2.6	No	Nonsense	c.244C>T in exon 4	p.Gln82*	NA	Wang et al. (2020)
16	1	2	No	Yes	-3.0	No	Deletion	E10-E16 del (deletion from intron 9 to 3' UTR)	NA	Yes	Lv et al. (2017)
17	1	2.5	Yes	Yes	-3.5 ^c	Yes	Frameshift	c.1096_1100del/AACTT in exon 10	p. Asn366Serfs*5	Yes	Costantini, et al. (2018))
18	2	NA	Yes	NA	-5.6 to -4.2	Yes	Missense	c.1103C>A in exon 10	p.A368D	NA	Nishi et al. (2016)
19	2	NA	Yes	Yes	-3.1	NA	Duplication	g.114,848,381_114,860,880dup	NA	Yes	Costantini, et al. (2018))
20	1	13	Yes	Yes	-2.3	NA	Frameshift	c.1206dup in exon 11 ^d	p.Val403Argfs7	NA	Collet C et al. (2018)
21	1	18	Yes	Yes	-3.9	NA	Missense	c.1876G>A in exon 18 ^d	p.Gly626Arg	NA	Collet C et al. (2018)
22	1	9-10	Yes	Yes	-4.1	Yes	Nonsense	c.766C>T in exon 8	p.Arg256*	Yes	Kämpe et al. (2017)
23	1	6	Yes	Yes	-1.2	Yes	Nonsense	c.745G>T in exon 7	p.E249*	NA	Chen et al. (2018)
24	1	4	Yes	No	-1.8	Yes	Splice-site	c.892-1G>A in intron 8	NA	NA	Cao et al. (2019)
25	2	6-12	Yes	Variable/1	-0.2 to -2.0	Yes	Frameshift	c.1106_1107insGAAA in exon 10	p.Phe369Leufs*5	Yes	This study

Abbreviations: BPs, bisphosphonates; NA, not available; OL, osteogenesis imperfecta; OP, osteoporosis; VCFs, vertebral compression fractures.

^aHaving one of the following typical extraskelletal manifestations marked "Yes": blue sclerae, dentinogenesis imperfecta, joint hypermobility, and hearing loss.

^bAge of the proband at the first fracture

^cBMD Z-score of the lumbar spine L2-L4

^d*PLS3* (18 exons, NG_012518) for exon numbering and the intronic region.

4 | DISCUSSION

We identified a Chinese family with X-linked OI caused by a novel frameshift mutation in *PLS3* (c.1106_1107insGAAA) for the first time. The proband presented with low bone mass, extremity fracture, and severe VCFs, whereas his brother had recurrent extremity fractures. Sanger sequencing confirmed that the two boys were hemizygous, and their mother was heterozygous for this mutation. All affected patients had blue sclerae, the only extraskeletal manifestation.

Previous and current findings suggested that the phenotype of the *PLS3* mutation consisted of low BMD, recurrent fractures, and less frequent extraskeletal manifestations, such as joint hypermobility, blue sclerae, hearing loss, and dentinogenesis imperfecta. *PLS3* has an important role in the development of neuromuscular junctions, and abnormal expression of *PLS3* might also contribute to the altered gait pattern (Ackermann et al., 2013). Moreover, zebrafish with *PLS3* knockdown showed deformed muscles, and increased muscle fiber size was observed in *PLS3*-overexpressing mice (van Dijk et al., 2013), indicating a potential role of *PLS3* in muscles. Some patients had epilepsy and ASD, indicating that neural symptoms might also be part of the phenotypic spectrum of the disease (Bourgeron, 2015; Stouffer et al., 2016). In general, peripheral fractures and VCFs were common in patients with *PLS3* mutations, which seemed to be clinical hallmarks and the first symptom of the disorder. Extraskeletal manifestations of *PLS3* mutations were uncommon.

In our study and previous research, heterozygous female patients generally had milder symptoms than did hemizygous males. *PLS3* is located on the X chromosome. Variability in X inactivation might account for the phenomenon and may also explain why a young girl with a de novo hemizygous *PLS3* mutation showed severe clinical symptoms (Connallon & Clark, 2013). The mutant allele in this girl was possibly located on the active X chromosome (Connallon & Clark, 2013). A recent study suggested that *PLS3* polymorphisms were associated with postmenopausal osteoporosis, suggesting that *PLS3* may serve as a genetic risk factor for osteoporosis (Shao et al., 2019). Overall, if recurrent low-impact fractures or VCFs occur in patients with an X chromosomal inheritance pattern, screening for a mutation in *PLS3* should be considered for early diagnosis and precise treatment.

Patients with low BMD and fractures are usually diagnosed with idiopathic osteoporosis. With the rapid development of gene sequencing technology, *PLS3* mutations have been identified in these patients. Interestingly, no hotspot mutations seemed to be found in the *PLS3* gene based on current data. In accordance with most previous studies, the mutation in *PLS3* in our study was predicted to cause elimination of its aberrant transcripts targeted by NMD. However, the production of *PLS3* detected in dermal fibroblasts of patients with *PLS3* mutation may be normal or decreased,

implying that this disorder was mainly caused by abnormalities in the structure and function of *PLS3* protein rather than *PLS3* deficiency (van Dijk et al., 2013; Wang et al., 2018).

The mechanism of the mutations in *PLS3* leading to OI remains elusive. *PLS3* is an actin-bundling protein that is evolutionarily conserved and widely expressed in a variety of organs. *PLS3* has been postulated to function at different stages of skeletal development. Fimbrin, an actin-bundling protein in chicks, was reported to be involved in the mechanosensory capability of osteocytes. As its homologous protein, *PLS3* may share a similar role (van Dijk et al., 2013; Kamioka et al., 2004; Tanaka-Kamioka et al., 1998). An additional study identified altered expression of osteocyte-specific proteins and a high level of osteocyte apoptosis in patients with *PLS3* mutations (Wesseling-Perry et al., 2017). Osteocytes are essential for maintaining bone homeostasis (Pathak et al., 2020). *PLS3* mutations may impair osteocytic function, which may further lead to an imbalance between osteoblast and osteoclast activity and cause the disease. *PLS3* also affected osteoblast differentiation by influencing the concentrations of intracellular calcium (Wang et al., 2018). A study indicated that *PLS3* can inhibit the maturity of osteoclasts by interacting with NF κ B-repressing factor (NKRF), further reducing the expression of nuclear factor of activated T cells 1 (Nfatc1), a pivotal molecule in promoting osteoclastogenesis (Neugebauer et al., 2018). *PLS3*-knockout mice exhibited upregulated transcription of NFATC1 and increased bone loss (Neugebauer et al., 2018). Thinner cortical bone was observed in *PLS3*-knockout mice due to the possibly reduced expression of Sfrp4, an important factor for stabilizing cortical bone thickness (Yorgan et al., 2020). In vitro, *PLS3* was related to bone mineralization. However, the effects of *PLS3* mutation on human bone remain controversial. Histomorphometric results revealed a decreased mineral apposition rate or an increased mineralization lag time in some patients with *PLS3* mutation, while another study found a normal deposition rate even with a low osteoid maturation time (Fahiminiya et al., 2014; Kampe et al., 2017; Laine et al., 2015). X-linked OI induced by *PLS3* mutation is very rare, and only a few reports are available on the histological features; thus, clarifying the underlying mechanism is difficult.

After once-yearly intravenous infusion of zoledronic acid, improvement in BMD, decreases in bone resorption markers, and reshaping of compressed vertebral bodies were observed in the proband and his brother. In a previous study, one female and two male patients with *PLS3* mutation were given teriparatide to promote bone formation (Valimaki et al., 2017). After 24-month treatment with teriparatide, all patients showed a minor increase in BMD without new clinical fractures (Valimaki et al., 2017). Larger longitudinal observational and interventional studies are needed to explore effective therapies for these patients.

Our study identified a family with X-linked OI induced by a novel *PLS3* gene mutation (c.1106_1107insGAAA), which further expanded the phenotype and genotype profile of X-linked OI. Some limitations exist in our study. First, considering the invasiveness of bone biopsy, histological analysis of our patients was absent in the study. Furthermore, in-depth studies on the possible pathogenesis are lacking. The long-term efficiency and safety of BP treatment in X-linked OI patients still need to be further affirmed owing to the short-term follow-up.

In conclusion, recurrent fractures were clinical hallmarks of X-linked OI caused by *PLS3* mutations. BP treatments may be helpful for increasing BMD in these patients. However, the correlation between *PLS3* mutations and phenotypes needs to be further investigated. The roles of *PLS3* in bone homeostasis remain to be clarified.

ACKNOWLEDGMENTS

This study was funded by the National Natural Science Foundation of China (No. 81873668), Beijing Natural Science Foundation (7202153), Chinese Academy of Medical Sciences Innovative Fund for Medical Sciences (CIFMS) (2016-I2M-3-003), and the National Key Research and Development Program of China (2018YFA0800801). We appreciated the proband with *PLS3* mutation and his family members for participation in this research.

CONFLICT OF INTEREST

Jing Hu, Lu-jiao Li, Wen-bin Zheng, Di-chen Zhao, Ou Wang, Yan Jiang, Xiao-ping Xing, Mei Li, and Weibo Xia declare that they have no conflict of interest.

AUTHOR CONTRIBUTIONS

J.H. and L.J.L. analyzed the data and wrote the manuscript. W.B.Z. and D.C.Z. contributed to data collection. O.W., Y.J., X.P.X., and W.B.X. contributed to review the manuscript. M.L. contributed to the conception and design of the research, acquisition, and interpretation of the data, and revised the manuscript.

ORCID

Mei Li  <https://orcid.org/0000-0002-4380-3511>

REFERENCES

- Ackermann, B., Kröber, S., Torres-Benito, L., Borgmann, A., Peters, M., Hosseini Barkoobe, S. M., Tejero, R., Jakubik, M., Schreml, J., Milbradt, J., Wunderlich, T. F., Riessland, M., Tabares, L., & Wirth, B. (2013). Plastin 3 ameliorates spinal muscular atrophy via delayed axon pruning and improves neuromuscular junction functionality. *Human Molecular Genetics*, 22(7), 1328–1347. <https://doi.org/10.1093/hmg/dd5540>
- Balasubramanian, M., Fratzi-Zelman, N., O'Sullivan, R., Bull, M., Fa Peel, N., Pollitt, R. C., Jones, R., Milne, E., Smith, K., Roschger, P., Klaushofer, K., Bishop, N. J., & Bishop, N. J. (2018). Novel *PLS3* variants in X-linked osteoporosis: Exploring bone material properties. *American Journal of Medical Genetics. Part A*, 176(7), 1578–1586. <https://doi.org/10.1002/ajmg.a.38830>
- Bardai, G., Ward, L. M., Trejo, P., Moffatt, P., Glorieux, F. H., & Rauch, F. (2017). Molecular diagnosis in children with fractures but no extraskelatal signs of osteogenesis imperfecta. *Osteoporosis International*, 28(7), 2095–2101. <https://doi.org/10.1007/s00198-017-4031-2>
- Besio, R., Chow, C. W., Tonelli, F., Marini, J. C., & Forlino, A. (2019). Bone biology: Insights from osteogenesis imperfecta and related rare fragility syndromes. *FEBS Journal*, 286(15), 3033–3056. <https://doi.org/10.1111/febs.14963>
- Bourgeron, T. (2015). From the genetic architecture to synaptic plasticity in autism spectrum disorder. *Nature Reviews Neuroscience*, 16(9), 551–563. <https://doi.org/10.1038/nrn3992>
- Cao, Y. J., Zhang, H., & Zhang, Z. L. (2019). Novel mutations in the *Wnt1*, *Tmem38b*, *P4hb*, and *Pls3* genes in four unrelated Chinese families with osteogenesis imperfecta. *Endocrine Practice*, 25(3), 230–241. <https://doi.org/10.4158/EP-2018-0443>
- Chen, T., Wu, H., Zhang, C., Feng, J., Chen, L., Xie, R., Wang, F., Chen, X., Zhou, H., Sun, H., & Xiao, F. (2018). Clinical, genetics, and bioinformatic characterization of mutations affecting an essential region of *PLS3* in patients with BMND18. *International Journal of Endocrinology*, 2018, 8953217. <https://doi.org/10.1155/2018/8953217>
- Collet, C., Ostertag, A., Ricquebourg, M., Delecourt, M., Tueur, G., Isidor, B., Guillot, P., Schaefer, E., Javier, R.-M., Funck-Brentano, T., Orcel, P., Laplanche, J.-L., & Cohen-Solal, M. (2018). Primary osteoporosis in young adults: Genetic basis and identification of novel variants in causal genes. *JBMR Plus*, 2(1), 12–21. <https://doi.org/10.1002/jbm4.10020>
- Connallon, T., & Clark, A. G. (2013). Sex-differential selection and the evolution of X inactivation strategies. *PLoS Genetics*, 9(4), e1003440. <https://doi.org/10.1371/journal.pgen.1003440>
- Costantini, A., Krallis, P., Kampe, A., Karavitakis, E. M., Taylan, F., Makitie, O., & Doulgeraki, A. (2018). A novel frameshift deletion in *PLS3* causing severe primary osteoporosis. *Journal of Human Genetics*, 63(8), 923–926. <https://doi.org/10.1038/s10038-018-0472-5>
- Costantini, A., Sarp, S., Kämpe, A., Mäkitie, R. E., Pettersson, M., Männikkö, M., Jiao, H., Taylan, F., Lindstrand, A., & Mäkitie, O. (2018). Rare copy number variants in array-based comparative genomic hybridization in early-onset skeletal fragility. *Frontiers in Endocrinology*, 9, 380. <https://doi.org/10.3389/fendo.2018.00380>
- Delanote, V., Vandekerckhove, J., & Gettemans, J. (2005). Plastins: Versatile modulators of actin organization in (patho)physiological cellular processes. *Acta Pharmacologica Sinica*, 26(7), 769.
- Fahiminiya, S., Majewski, J., Al-Jallad, H., Moffatt, P., Mort, J., Glorieux, F. H., Roschger, P., Klaushofer, K., & Rauch, F. (2014). Osteoporosis caused by mutations in *PLS3*: Clinical and bone tissue characteristics. *Journal of Bone and Mineral Research*, 29(8), 1805–1814. <https://doi.org/10.1002/jbmr.2208>
- Folkestad, L., Hald, J. D., Canudas-Romo, V., Gram, J., Hermann, A. P., Langdahl, B., Abrahamsen, B. O., & Brixen, K. (2016). Mortality and causes of death in patients with osteogenesis imperfecta: A register-based nationwide cohort study. *Journal of Bone and Mineral Research*, 31(12), 2159–2166. <https://doi.org/10.1002/jbmr.2895>
- Genant, H. K., Wu, C. Y., van Kuijk, C., & Nevitt, M. C. (1993). Vertebral fracture assessment using a semiquantitative technique.

- Journal of Bone and Mineral Research*, 8(9), 1137–1148. <https://doi.org/10.1002/jbmr.5650080915>
- Kamioka, H., Sugawara, Y., Honjo, T., Yamashiro, T., & Takano-Yamamoto, T. (2004). Terminal differentiation of osteoblasts to osteocytes is accompanied by dramatic changes in the distribution of actin-binding proteins. *Journal of Bone and Mineral Research*, 19(3), 471–478. <https://doi.org/10.1359/JBMR.040128>
- Kampe, A. J., Costantini, A., Levy-Shraga, Y., Zeitlin, L., Roschger, P., Taylan, F., Lindstrand, A., Paschalis, E. P., Gamsjaeger, S., Raas-Rothschild, A., & Makitie, O. (2017). PLS3 deletions lead to severe spinal osteoporosis and disturbed bone matrix mineralization. *Journal of Bone and Mineral Research*, 32(12), 2394–2404. <https://doi.org/10.1002/jbmr.3233>
- Kämpe, A. J., Costantini, A., Mäkitie, R. E., Jäntti, N., Valta, H., Mäyränpää, M., Kröger, H., Pekkinen, M., Taylan, F., Jiao, H., & Mäkitie, O. (2017). PLS3 sequencing in childhood-onset primary osteoporosis identifies two novel disease-causing variants. *Osteoporosis International*, 28(10), 3023–3032. <https://doi.org/10.1007/s00198-017-4150-9>
- Kannu, P., Mahjoub, A., Babul-Hirji, R., Carter, M. T., & Harrington, J. (2017). PLS3 mutations in X-linked osteoporosis: Clinical and bone characteristics of two novel mutations. *Hormone Research in Paediatrics*, 88(3–4), 298–304. <https://doi.org/10.1159/000477242>
- Khadilkar, A. V., Sanwalka, N. J., Chiplonkar, S. A., Khadilkar, V. V., & Mughal, M. Z. (2011). Normative data and percentile curves for Dual Energy X-ray Absorptiometry in healthy Indian girls and boys aged 5–17 years. *Bone*, 48(4), 810–819. <https://doi.org/10.1016/j.bone.2010.12.013>
- Laine, C. M., Wessman, M., Toiviainen-Salo, S., Kaunisto, M. A., Mayranpää, M. K., Laine, T., Pekkinen, M., Kröger, H., Välimäki, V.-V., Välimäki, M. J., Lehesjoki, A.-E., & Makitie, O. (2015). A novel splice mutation in PLS3 causes X-linked early onset low-turnover osteoporosis. *Journal of Bone and Mineral Research*, 30(3), 510–518. <https://doi.org/10.1002/jbmr.2355>
- Li, H., Ji, C. Y., Zong, X. N., & Zhang, Y. Q. (2009). Height and weight standardized growth charts for Chinese children and adolescents aged 0 to 18 years. *Zhonghua Er Ke Za Zhi*, 47(7), 487–492.
- Lv, F., Ma, M., Liu, W., Xu, X., Song, Y., Li, L., Jiang, Y., Wang, O., Xia, W., Xing, X., Qiu, Z., & Li, M. (2017). A novel large fragment deletion in PLS3 causes rare X-linked early-onset osteoporosis and response to zoledronic acid. *Osteoporosis International*, 28(9), 2691–2700. <https://doi.org/10.1007/s00198-017-4094-0>
- Marini, J. C., Forlino, A., Bächinger, H. P., Bishop, N. J., Byers, P. H., Paeppe, A. D., Fassier, F., Fratzl-Zelman, N., Kozloff, K. M., Krakow, D., Montpetit, K., & Semler, O. (2017). Osteogenesis imperfecta. *Nature Reviews Disease Primers*, 3, 17052. <https://doi.org/10.1038/nrdp.2017.52>
- Neugebauer, J., Heilig, J., Hosseinbarkooie, S., Ross, B. C., Mendoza-Ferreira, N., Nolte, F., Peters, M., Hölker, I., Hupperich, K., Tschanz, T., Grysko, V., Zaucke, F., Niehoff, A., & Wirth, B. (2018). Plastin 3 influences bone homeostasis through regulation of osteoclast activity. *Human Molecular Genetics*, 27(24), 4249–4262. <https://doi.org/10.1093/hmg/ddy318>
- Nishi, E., Masuda, K., Arakawa, M., Kawame, H., Kosho, T., Kitahara, M., Kubota, N., Hidaka, E., Katoh, Y., Shirahige, K., & Izumi, K. (2016). Exome sequencing-based identification of mutations in non-syndromic genes among individuals with apparently syndromic features. *American Journal of Medical Genetics. Part A*, 170(11), 2889–2894. <https://doi.org/10.1002/ajmg.a.37826>
- Pathak, J. L., Bravenboer, N., & Klein-Nulend, J. (2020). The osteocyte as the new discovery of therapeutic options in rare bone diseases. *Frontiers in Endocrinology*, 11, 405. <https://doi.org/10.3389/fendo.2020.00405>
- Richards, C. S., Bale, S., Bellissimo, D. B., Das, S., Grody, W. W., Hegde, M. R., Lyon, E., & Ward, B. E. (2008). ACMG recommendations for standards for interpretation and reporting of sequence variations: Revisions 2007. *Genetics in Medicine*, 10(4), 294–300. <https://doi.org/10.1097/GIM.0b013e31816b5cae>
- Shao, C., Wang, Y. W., He, J. W., Fu, W. Z., Wang, C., & Zhang, Z. L. (2019). Genetic variants in the PLS3 gene are associated with osteoporotic fractures in postmenopausal Chinese women. *Acta Pharmacologica Sinica*, 40(9), 1212–1218. <https://doi.org/10.1038/s41401-019-0219-7>
- Song, P., Li, X., Gasevic, D., Flores, A. B., & Yu, Z. (2016). BMI, waist circumference reference values for Chinese school-aged children and adolescents. *International Journal of Environmental Research and Public Health*, 13(6), E589. <https://doi.org/10.3390/ijerp13060589>
- Stouffer, M. A., Golden, J. A., & Francis, F. (2016). Neuronal migration disorders: Focus on the cytoskeleton and epilepsy. *Neurobiology of Disease*, 92(Pt A), 18–45. <https://doi.org/10.1016/j.nbd.2015.08.003>
- Tanaka-Kamioka, K., Kamioka, H., Ris, H., & Lim, S. S. (1998). Osteocyte shape is dependent on actin filaments and osteocyte processes are unique actin-rich projections. *Journal of Bone and Mineral Research*, 13(10), 1555–1568. <https://doi.org/10.1359/jbmr.1998.13.10.1555>
- Tauer, J. T., Robinson, M. E., & Rauch, F. (2019). Osteogenesis imperfecta: New perspectives from clinical and translational research. *JBMR Plus*, 3(8), e10174. <https://doi.org/10.1002/jbmr.4.10174>
- Valimäki, V. V., Makitie, O., Pereira, R., Laine, C., Wesseling-Perry, K., Maatta, J., Kirjavainen, M., Viljakainen, H., & Valimäki, M. J. (2017). Teriparatide treatment in patients With WNT1 or PLS3 mutation-related early-onset osteoporosis: A pilot study. *Journal of Clinical Endocrinology and Metabolism*, 102(2), 535–544. <https://doi.org/10.1210/je.2016-2423>
- van Dijk, F. S., Zillikens, M. C., Micha, D., Riessland, M., Marcellis, C. L., de Die-Smulders, C. E., Milbradt, J., Franken, A. A., Harsevoort, A. J., Lichtenbelt, K. D., & Pals, G. (2013). PLS3 mutations in X-linked osteoporosis with fractures. *New England Journal of Medicine*, 369(16), 1529–1536. <https://doi.org/10.1056/NEJMoa1308223>
- Wang, L., Bian, X., Cheng, G., Zhao, P., Xiang, X., Tian, W., Li, T., & Zhai, Q. (2020). A novel nonsense variant in PLS3 causes X-linked osteoporosis in a Chinese family. *Annals of Human Genetics*, 84(1), 92–96. <https://doi.org/10.1111/ahg.12344>
- Wang, L., Zhai, Q., Zhao, P., Xiang, X., Zhang, X., Tian, W., & Li, T. (2018). Functional analysis of p.Ala253_Leu254insAsn mutation in PLS3 responsible for X-linked osteoporosis. *Clinical Genetics*, 93(1), 178–181. <https://doi.org/10.1111/cge.13081>
- Webb, E. A., Balasubramanian, M., Fratzl-Zelman, N., Cabral, W. A., Titheradge, H., Alsaedi, A., Saraff, V., Vogt, J., Cole, T., Stewart, S., Crabtree, N. J., Sargent, B. M., Gamsjaeger, S., Paschalis, E. P., Roschger, P., Klaushofer, K., Shaw, N. J., Marini, J. C., & Högl, W. (2017). Phenotypic spectrum in osteogenesis imperfecta due to mutations in TMEM38B: Unraveling a complex cellular defect.

Journal of Clinical Endocrinology and Metabolism, 102(6), 2019–2028. <https://doi.org/10.1210/jc.2016-3766>

Wesseling-Perry, K., Mäkitie, R. E., Välimäki, V.-V., Laine, T., Laine, C. M., Välimäki, M. J., Pereira, R. C., & Mäkitie, O. (2017). Osteocyte protein expression is altered in low-turnover osteoporosis caused by mutations in WNT1 and PLS3. *Journal of Clinical Endocrinology and Metabolism*, 102(7), 2340–2348. <https://doi.org/10.1210/jc.2017-00099>

Yorgan, T. A., Sari, H., Rolvien, T., Windhorst, S., Failla, A. V., Kornak, U., Oheim, R., Amling, M., & Schinke, T. (2020). Mice lacking

plastin-3 display a specific defect of cortical bone acquisition. *Bone*, 130, 115062. <https://doi.org/10.1016/j.bone.2019.115062>

How to cite this article: Hu J, Li Lj, Zheng Wb, et al. A novel mutation in *PLS3* causes extremely rare X-linked osteogenesis imperfecta. *Mol Genet Genomic Med*. 2020;8:e1525. <https://doi.org/10.1002/mgg3.1525>